Aust. J. Phys., 1989, **42**, 267–87

Time-dependent Studies of Optical Bistability in Atomic Sodium

W. E. Schulz,[A] *W. R. MacGillivray and M. C. Standage*

Division of Science and Technology, Griffith University,
Nathan, Qld 4111, Australia.
[A] Present address: Sektion Physik der Universität München,
D-8046 Garching, West Germany.

Abstract

A bistable system consisting of an optical cavity with a medium of sodium atomic beams has been subjected to square pulses of light resonant with a D transition. The lifetimes of the field in the cavity and of the atomic medium are approximately equal. The system transmission data recorded has been compared with simulated data calculated from a theoretical model which treats the atomic energy configuration associated with the D lines as a three-level, lambda-type. Good qualitative agreement is obtained showing the system switching on to the high transmission branch. In particular, as the intensity of the input pulse tends, from the high intensity side, to the low to high branch transition threshold, switching is delayed by a time which is more than one order of magnitude longer than the field and atomic lifetimes.

1. Introduction

Ever since the prediction (Szöke *et al.* 1969; McCall 1974) and first demonstration (Gibbs *et al.* 1976) of optical bistability, this phenomenon has created widespread interest. The bistable behaviour arises when part of the electromagnatic field, after nonlinear interaction with a suitable medium, is fed back into the medium. Hence the transmitted field does not depend solely on the interaction of the injected field and the medium but also on the history of the interaction stored in the feedback. This memory effect can, under appropriate conditions, lead to two (or more) stable output states for a given input, hence the term 'bistability'. The analogy of this system with an electronic Schmitt–Trigger circuit, and its potential for optical data processing and storage, has spurred research into the applications of the effect (see for example Smith *et al.* 1987).

At a more fundamental level, optical bistability has enabled the study of a nonlinear system far from equilibrium. A large amount of literature now exists on the topic and a good overview of the field can be obtained from the book by Gibbs (1985).

Atomic sodium was employed as the medium inside a Fabry–Perot etalon in the first reported experiments (Gibbs *et al.* 1976) and it has continued as a popular choice since, due to the convenient wavelengths of its D lines and their saturability at weak intensity. However, these transitions are between energy levels with complicated hyperfine structure. Two experimental techniques

0004-9506/89/030267$03.00

have been used to minimise the effects due to the hyperfine structure and to simplify analysis. In the first method, sodium was evaporated in a heated cell along with a noble gas (Sandle and Gallagher 1981). The width of the atomic line was dominated by pressure broadening and, in the case of the D_1 line, could be interpreted as a $J'_{1/2} \rightarrow J_{1/2}$ transition (Ballagh *et al.* 1981). The number of participating states was further reduced in other experiments by optically pumping the pressure-broadened transition in the presence of a magnetic field (Arecchi *et al.* 1982; Mlynek *et al.* 1984). Various manifestations of steady-state and dynamic optical bistability (and tristability) were studied using this approach.

The second method is more elaborate and involves the use of atomic beams of sodium at right angles to the direction of propagation of the cavity field. This configuration reduces the Doppler width of the transitions to a degree dependent on the collimation of the beams. To maintain an atomic density sufficiently high for the system to exhibit bistability, a linear array of beams is required. In the first such experiment, 50 atomic beams with a residual Doppler width of 15 MHz formed the medium of a high Q optical cavity (Weyer *et al.* 1981). Irradiation with σ^+ polarised light tuned to resonance with the $3^2S_{1/2}(F'=2) \rightarrow 3^2P_{3/2}(F=3)$ transition of the D_2 line reduced the participating atomic levels effectively to two (Abate 1974). This experiment concentrated on absorptive bistability and even though a slow laser intensity cycle was used, significant deviations from steady-state behaviour were observed.

The most extensive experimental studies of bistability using sodium atomic beams as the intracavity medium have been performed by Kimble's group at the University of Texas. Again, high Q optical cavities have been used and the atoms prepared in two levels by optical pumping before reaching the cavity. They have made careful comparisons between experimental data and theory for steady-state and transient behaviour in absorptive bistability (Grant and Kimble 1982, 1983; Kimble *et al.* 1983; Rosenberger *et al.* 1983, 1984) and steady-state bistability in a mixed absorptive-dispersive regime (Orozco *et al.* 1987*a*). A detailed study of the role of the transverse structure of the intracavity field has also been undertaken (Orozco *et al.* 1987*b*). An intrinsic dynamical instability on the upper branch has been observed (Orozco *et al.* 1984), and recently, squeezed-state generation in the bistable system has been reported (Raizen *et al.* 1987; Orozco *et al.* 1987*c*).

The two experiments described above involving atomic beams employed optical cavities of high finesse. In both cases, the cavity lifetime was two orders of magnitude greater than the atomic lifetime and hence the response of the system was governed by the cavity. The work reported here is of a study of the response of a bistable system where the cavity and atomic lifetimes are approximately equal. Cavity finesse and hence lifetime is reduced by employing mirrors with reflectivities substantially less than one. To maintain the system in the bistable regime, this reduction in reflectivity must be compensated for by increasing the atomic density. This can only be obtained by lowering the collimation ratio of the atomic beams and hence increasing the residual Doppler width. For the experiment described here, the absorption spectrum of the D lines was such as to resolve the hyperfine structure of the $3^2S_{1/2}$ ground state but not the 3^2P upper levels. Hence, no attempt was made to optically

pump the atoms to two-level systems. Rather, the energy configuration was modelled as a lambda-type three-level system (Orriols 1979).

In Section 2, the theory for the response of a low finesse cavity filled with a medium of the three-level atoms is developed. The apparatus and the experimental procedures are described in Section 3, while the results of the experiment are presented in Section 4 where they are compared with the calculations from the theory. The work is summarised and conclusions drawn in Section 5.

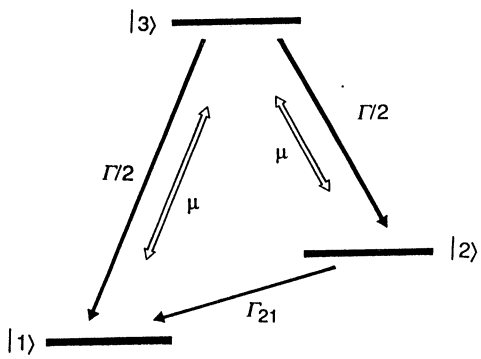

Fig. 1. Lambda-type three-level description of the energy states associated with a sodium D transition.

2. Theory

The theory of optical bistability is now well developed. A comprehensive overview can be found in the literature (see for example Lugiato 1983; Abraham and Smith 1982; Gibbs 1985) so only a very brief outline is given here with emphasis on experimentally relevant details. The three-state model for the sodium D lines is shown in Fig. 1. The separation of the two ground states corresponds to the hyperfine splitting of the $F' = 1$ and $F' = 2$ states of the $3^2S_{1/2}$ level and is 1772 MHz. The ground states are both radiatively coupled to the excited state $|3\rangle$ with equal dipole moments μ. It is assumed that there is equal probability of $|3\rangle$ relaxing to state $|2\rangle$ or state $|1\rangle$. A coupling Γ_{21} of the two ground states is included to account for a redistribution due to atoms entering and leaving the interaction region. No relaxations are allowed out of the system. The relaxation rate Γ is written in terms of the usual atomic lifetimes as $\Gamma = 1/T_1 = 2/T_2$. Similarly, a ground state redistribution lifetime τ is defined as $\Gamma_{21} = 1/\tau$. No polarisation effects are included. This simple model for these sodium transitions has been shown to be quite suitable under conditions where broadening due to the Doppler effect dominates collisional broadening (Orriols 1979; Pegg and Schulz 1985; Schulz *et al.* 1987). Under experimental conditions described in the next section, where the two ground hyperfine states are resolved in a collision-free regime, the three-state model should be even more suitable.

The response of the atoms can be described using the density operator:

$$i\hbar\dot{\rho} = [H, \rho] + \text{relaxation terms}, \tag{1}$$

where H is the semiclassical Hamiltonian for the system. In the rotating-wave approximation, the component equations for the three-state atomic system are

given by (Orriols 1979)

$$\dot{\rho}_{33} = -2\mathrm{Im}\,(\alpha\tilde{\rho}_{13}) - 2\mathrm{Im}\,(\alpha\tilde{\rho}_{23}) - \Gamma\rho_{33}\,,$$

$$\dot{\rho}_{22} = 2\mathrm{Im}\,(\alpha\tilde{\rho}_{23}) + \Gamma_{21}(\rho_{11} - \rho_{22}) + \tfrac{1}{2}\Gamma\rho_{33}\,,$$

$$\dot{\rho}_{11} = 2\,\mathrm{Im}(\alpha\tilde{\rho}_{13}) - \Gamma_{21}(\rho_{11} - \rho_{22}) + \tfrac{1}{2}\Gamma\rho_{33}\,,$$

$$\dot{\tilde{\rho}}_{13} = -(\tfrac{1}{2}\Gamma + \mathrm{i}\Delta)\tilde{\rho}_{13} - \mathrm{i}\,\alpha^*(\rho_{11} - \rho_{33}) - \mathrm{i}\,\alpha^*\rho_{12}\,,$$

$$\dot{\tilde{\rho}}_{23} = -(\tfrac{1}{2}\Gamma + \mathrm{i}\Delta')\tilde{\rho}_{23} - \mathrm{i}\,\alpha^*(\rho_{22} - \rho_{33}) - \mathrm{i}\,\alpha^*\rho_{21}\,,$$

$$\dot{\rho}_{12} = -\{\Gamma_{21} + \mathrm{i}(\Delta - \Delta')\}\rho_{12} + \mathrm{i}\,\alpha^*\tilde{\rho}_{32} - \mathrm{i}\,\alpha\tilde{\rho}_{13}\,,$$

$$\rho_{11} + \rho_{22} + \rho_{33} = 1\,, \tag{2}$$

where α is the half Rabi frequency,

$$\alpha = \mu E/2\hbar\,, \tag{3}$$

and where E is the amplitude of the electric field $\mathcal{E}$, propagating in the z direction with frequency ω_L,

$$\mathcal{E}(z,t) = \tfrac{1}{2}E(z,t)\,\exp\{\mathrm{i}(\omega_L t - kz)\} + \mathrm{c.c.} \tag{4}$$

The detuning terms, Δ and Δ', are defined as

$$\Delta = \omega_L - \omega_{31}\,, \qquad \Delta' = \omega_L - \omega_{32}\,, \tag{5a,b}$$

where ω_{31} (ω_{32}) is the frequency of the $|1\rangle - |3\rangle$ ($|2\rangle - |3\rangle$) transition. The usual transformation to the rotating frame for the off-diagonal elements ρ_{i3} has been made:

$$\rho_{i3} = \tilde{\rho}_{i3}\,\exp\{\mathrm{i}(\omega_L t - kz)\}\,. \tag{6}$$

The polarisation $\mathcal{P}$ induced in the medium is found to have the same form as the field, that is

$$\mathcal{P}(z,t) = \tfrac{1}{2}P(z,t)\,\exp\{\mathrm{i}(\omega_L t - kz)\} + \mathrm{c.c.}\,, \tag{7}$$

where

$$P(z,t) = 2N\mu\{\tilde{\rho}_{31}(z,t) + \tilde{\rho}_{32}(z,t)\}\,, \tag{8}$$

N being the atomic density.

The amplitude of the electric field $E(z,t)$ obeys Maxwell's equation in the slowly varying amplitude approximation (Allen and Eberly 1975):

$$\frac{\partial}{\partial z}E(z,t) + \frac{1}{c}\frac{\partial}{\partial t}E(z,t) = \frac{\mathrm{i}\,\omega_L}{2c\epsilon_0}P(z,t)\,. \tag{9}$$

Using (3) and (8), expression (9) becomes

$$\frac{\partial}{\partial z}\alpha(z,t)+\frac{1}{c}\frac{\partial}{\partial t}\alpha(z,t)=\frac{\mathrm{i}\Gamma T}{L}C\{\tilde{\rho}_{31}(z,t)+\tilde{\rho}_{32}(z,t)\}, \tag{10}$$

where C is the bistability parameter from two-state bistability theory defined as (Bonifacio and Lugiato 1976)

$$C=\alpha_{\mathrm{abs}}L/2T, \tag{11}$$

with α_{abs} the linear absorption coefficient

$$\alpha_{\mathrm{abs}}=\frac{\omega_L\mu^2N}{\hbar\epsilon_0 c\Gamma}. \tag{12}$$

The numerical value of C does not allow the same interpretation in the three-state model as in the two-state model. It is used in this work as a convenient, dimensionless measure of the atomic density.

The medium is assumed to fill the space between the input and output mirrors of the cavity. These mirrors are separated by length L, and each has the transmittivity T. As shown in Section 4, experiments with the linear cavity and the ring cavity yielded essentially similar results. Hence, the analytically simpler ring cavity is chosen to be included in the theoretical model. In this cavity, the light from the output mirror is fed back to the input mirror via one or more perfectly reflecting mirrors. The ring cavity imposes the boundary conditions (Lugiato 1983)

$$E(0,t)=T^{\frac{1}{2}}E_{\mathrm{i}}(t)+R\exp(-\mathrm{i}\Delta_{\mathrm{c}}\tau_{\mathrm{R}})E(L,t-\Delta t), \tag{13a}$$

$$E_{\mathrm{T}}(t)=T^{\frac{1}{2}}E(L,t), \tag{13b}$$

where Δ_{c} is the detuning of the cavity frequency ω_{c} from the laser frequency ω_L,

$$\Delta_{\mathrm{c}}=\omega_{\mathrm{c}}-\omega_{\mathrm{L}}, \tag{14}$$

while τ_{R} is the empty cavity round-trip time and is the inverse of the free spectral range (FSR). In equation (13a), Δt is the time taken for the field to travel around the ring from the output mirror ($z=L$) to the input mirror ($z=0$). The finesse of the cavity is given by

$$F=\pi R^{\frac{1}{2}}/T, \tag{15}$$

where R is the reflectivity of the input and output mirrors which are assumed to be absorptionless, so that

$$R+T=1. \tag{16}$$

The time evolution of the field and atomic variables is thus described by the two coupled partial differential equations (2) and (10) and a difference equation

imposed by the boundary conditions, together with the scaling condition of equation (3). Each one of the three equations describes a time evolution with a characteristic time scale: the atomic variable on the scale of the atomic decay times and the field variables by the propagation through the medium, the cavity round-trip time and, ultimately, the lifetime of the photon in the cavity. If the cavity and the atomic lifetimes differ significantly, then the complexity of the equations can be reduced significantly. For example, in the 'good cavity' limit, where the high reflectivity of the mirrors leads to a cavity lifetime much greater than that of the atoms, the atoms are considered to follow the field instantaneously and so the atomic variables can be eliminated adiabatically (see for example Bonifacio and Meystre 1978). However, in our experiment the two lifetimes are of the same order of magnitude and so no such simplification can be made.

For an empty cavity, the delay term $E(L,t-\Delta t)$ in the boundary condition (13a) can be expanded in a Taylor series around t. The internal field can be eliminated resulting in the differential equation

$$\frac{\partial E_T}{\partial t} = \kappa E_i \exp(i\Delta_c \tau_R) + \frac{R\kappa}{T}\{1 - (1/R)\exp(i\Delta_c \tau_R)\}E_T, \tag{17}$$

where the fields are now functions of the same time t, and

$$\kappa = T/R\tau_R. \tag{18}$$

For the cavity tuned to resonance, equation (17) becomes

$$\frac{\partial E_T}{\partial t} = \kappa E_i - \kappa E_T, \tag{19}$$

which is a simple gain/loss equation, and κ can thus be interpreted as the decay rate of the field inside the cavity. The cavity detuning leads to a 'ringing' at the difference frequency with the oscillations decaying with the cavity decay rate. This is illustrated in Fig. 2 where the transmitted intensity is shown as a function of time for various cavity detunings.

The solution of equations (2) and (10) together with the boundary conditions is not a straightforward numerical problem. A number of common differential equation solvers were tried without success. Numerical instabilities could be clearly recognised with the appearance of features such as rapid oscillations in the transmitted intensity or population terms which were negative. The set of equations require a very stable numerical algorithm, and we found the backward Euler algorithm to be the only suitable technique for this problem.

The significance of the difference between the atomic and cavity timescales can be seen in Fig. 3, a numerical simulation of the time evolution of the intensity transmitted by the system. The finesse is increased as depicted by the increase in R and decrease in T, while C is maintained at a constant value of 2 in order to remain outside the bistable regime. Both the injected field and cavity frequencies were set to the $|2\rangle$–$|3\rangle$ transition frequency. The FSR of the cavity was 1·2 GHz. The steady-state field inside the cavity was kept constant so that the Rabi frequency remained constant for easier comparison.

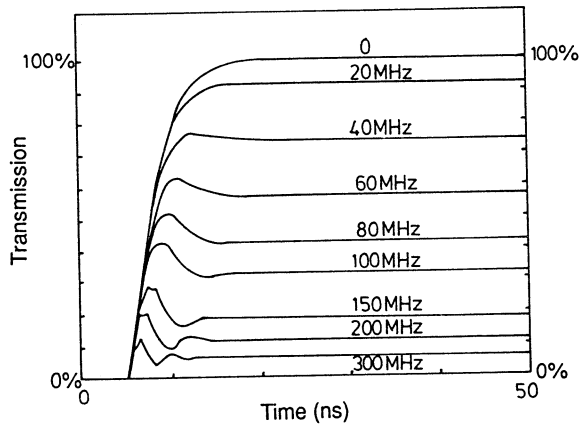

Fig. 2. Simulated response of an empty ring cavity for various cavity detunings to a light pulse switched on at $t = 5$ ns with a 1 ns rise time, where $R = 0 \cdot 7$, $T = 0 \cdot 3$ and FSR = $1 \cdot 2$ GHz.

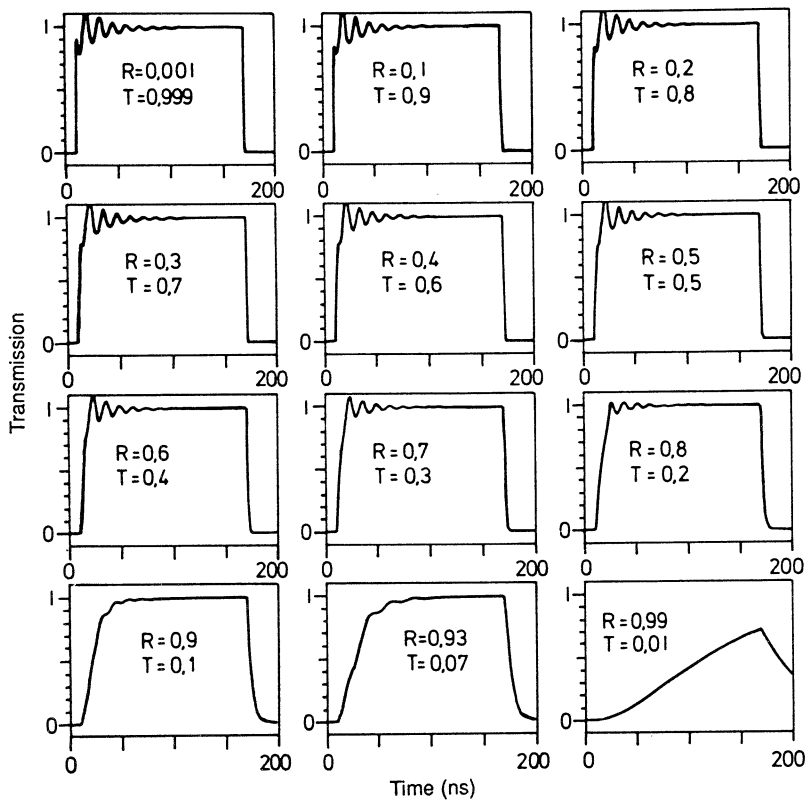

Fig. 3. Simulated response of a ring cavity with a sodium vapour medium to a light pulse with a rise time of $1 \cdot 5$ ns switched on at $t = 10$ ns and off at $t = 170$ ns, and where FSR = $1 \cdot 2$ GHz. The finesse of the cavity is increased from the top left to the bottom right, while the intracavity field and the C number are kept constant ($C = 2$). The Rabi oscillations disappear as the cavity filling time increases.

Specifically, the equivalent Rabi frequency of the incident field α_i was set to $0{\cdot}25T^{\frac{1}{2}}$ rad ns^{-1}. For these and all other calculations presented here, the relaxation rate Γ was taken as the appropriate sodium 3^2P value of 1/16 ns^{-1}, while Γ_{21} was chosen as 1 μs^{-1} which is deduced from the estimated transit time of an atom through the laser beam.

Doppler broadening was not included in any of the calculations. The dominant reason for this omission was the vast increase in computer time required to include it. As illustrated in Fig. 6 below, the residual width of the transitions due to Doppler broadening is less than 200 MHz. Since this value is comparable with the power broadened width for typical intracavity fields, the approximation is not as severe as may at first seem. However, neglect of Doppler broadening in the model meant that quantiative comparisons between experimental and theoretical data were not possible.

The plots in Fig. 3 show that in the 'bad cavity' limit, that is, very low cavity finesse, atomic optical nutations are quite clear. As the finesse increases, the nutations diminish until they disappear completely in the 'good cavity' limit where the cavity timescale dominates.

3. Apparatus and Experiment

The hyperfine splitting 1772 MHz between the $F' = 1$ and 2 states of the $3^2S_{1/2}$ ground state can create difficulties in the analysis of experiments carried out in sodium atomic vapours. The Doppler profiles of the two sets of transitions out of these hyperfine states to a 3^2P level overlap substantially in a vapour, and consequently complicating effects due to this three-level system can arise (Alzetta *et al.* 1979; Gawlik and Zachorowski 1987). The overlapping of these Doppler profiles also leads to markedly different behaviour in the transmissions of a ring cavity and a Fabry–Perot etalon with sodium vapour as the intracavity medium (Schulz *et al.* 1983; 1987). To enable the observation of the time response of a bistable system without the added complications of these overlapping profiles, the collimation ratio of the atomic beams had to be sufficiently large so that these transitions were resolved. On the other hand, the collimation ratio could not be so high that the low-finesse cavity system did not enter the bistable regime due to a too small atom density. From equations (10) and (12), as the transmittivity T of the mirrors is increased (lower finesse), so the atom density N must be increased to maintain constant C. The apparatus described here satisfied these conditions.

The apparatus configuration for the time response experiment is illustrated in Fig. 4. The radiation was produced by a Spectra-Physics 380 D actively stabilised ring dye laser pumped by a Spectra-Physics 171 Ar^+ laser. Up to 600 mW of single-mode light was available from this laser system with a jitter bandwidth of about 1 MHz. A pulse was created from the c.w. laser radiation by the electro-optic switch, a Lasermetrics Model 5016. The length of the pulse was adjustable between 2 and 480 ns and the rise time was measured to be of the order of 1 ns. The pulse was linearly polarised parallel to the direction of the atomic beams. The switch was triggered by a square wave generator at a rate of about 3 Hz. The time base of the storage oscilloscope was also triggered by this wave. Before injection into the vacuum chamber, the light pulse passed through a 1 mm aperture and a collimater.

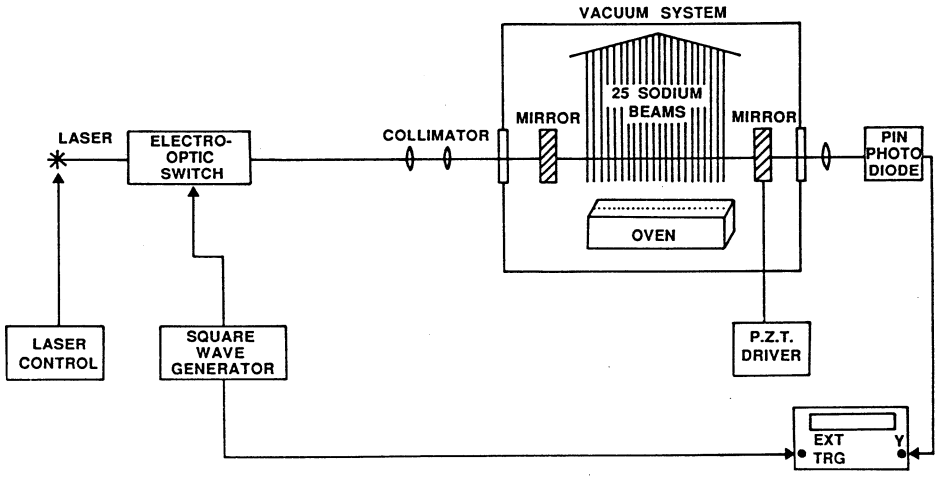

Fig. 4. Schematic of the apparatus.

The light transmitted by the cavity apparatus was detected by a PIN photodiode (HP5082-4420). The transmitted radiation was quite weak and normally, it had to be focussed onto the photodiode whose output was recorded on the storage oscilloscope, a Tektronix Model 7834 incorporating a Model 7B80 time base and a Model 7A24 dual channel amplifier with a specified bandwidth of 300 MHz and a rise time of 1·2 ns.

The central part of the experiment was the atomic beam system illustrated in Fig. 5. The system consisted of a vacuum tank made of 316 type non-magnetic steel which contained the atomic oven, a liquid nitrogen cold trap and the optical cavity mirrors. The bottom of the tank had two flanges, one for the pumping system and one for the oven assembly. The top lid including the cold trap could be lifted off the main chamber by a small crane and a winch. This allowed easy access to the mirror mounts, oven and cold trap. The pumping system consisted of an Edwards Diffstak 100/300 water-cooled oil diffusion pump backed by an Edwards E2M8 two-stage rotary pump. The base pressure in the tank was approximately 10^{-4} Pa. The cold trap consisted of a copper cylinder which encircled the oven. The trap was suspended from the bottom of the liquid nitrogen dewar. The dewar was filled through thin stainless steel bellows at the top. The glass windows, electrical feedthroughs and the ionisation gauge head were fitted to 40 mm diameter flanges. Mechanical linear motion feedthroughs, two per mirror mount, enabled the alignment of the optical cavity. Either a Fabry–Perot etalon of free spectral range 615 MHz or a three-mirror ring cavity of free spectral range 1230 MHz was employed. The two drives rotated the mount about the horizontal and vertical axis respectively. The mounts were designed to hold 25·4 mm diameter mirrors. One of the mirrors was mounted on a Burleigh Instruments PZ-80 piezo-electric translator which was driven by a Burleigh Instruments RC-42 Ramp Generator. All mirrors were hard-coated $\lambda/100$ surfaces with the input and output mirrors having a reflectivity of 93%. The finesse of each cavity with the laser light detuned from the medium resonance was about 10.

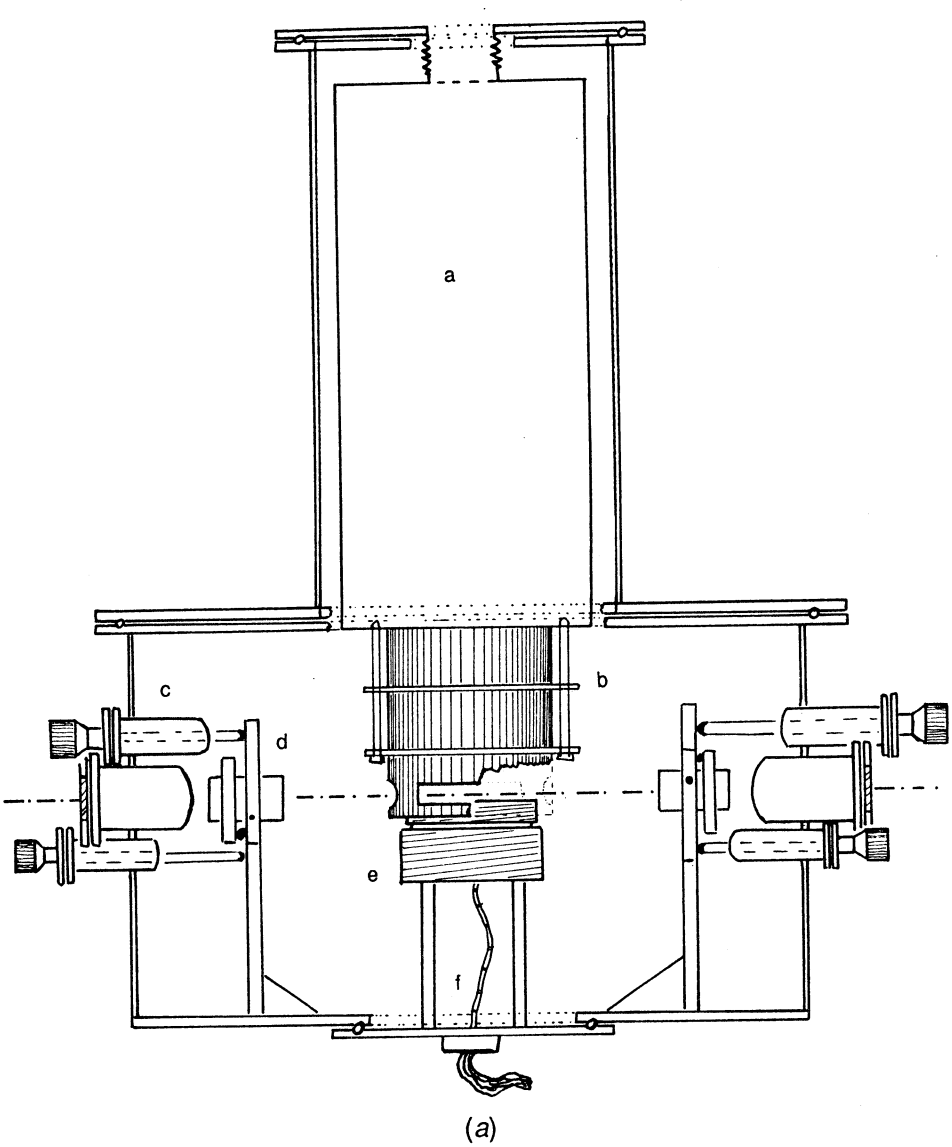

Fig. 5. Vacuum chamber containing atomic beam system and optical cavity: (*a*) side view: a—liquid nitrogen dewar; b—cold trap; c—mechanical feedthrough; d—mirror mount; e—oven assembly; f—electrical feedthrough. (*b*) top view: a—swing valve and Diffstak; b—ionisation gauge head; c—mechanical feedthrough; d—mirror mount; e—oven assembly; f—electrical feedthrough; g—optical port.

The two-stage atomic beam oven was machined from 316 stainless steel and topped by a copper mask containing a linear array of 25 holes. The direction of the array was along the line of the light propagation whereas each atomic beam was perpendicular to the light beam. Since the copper plate of the mask was rather thick (6 mm), the holes could not be drilled accurately. Instead

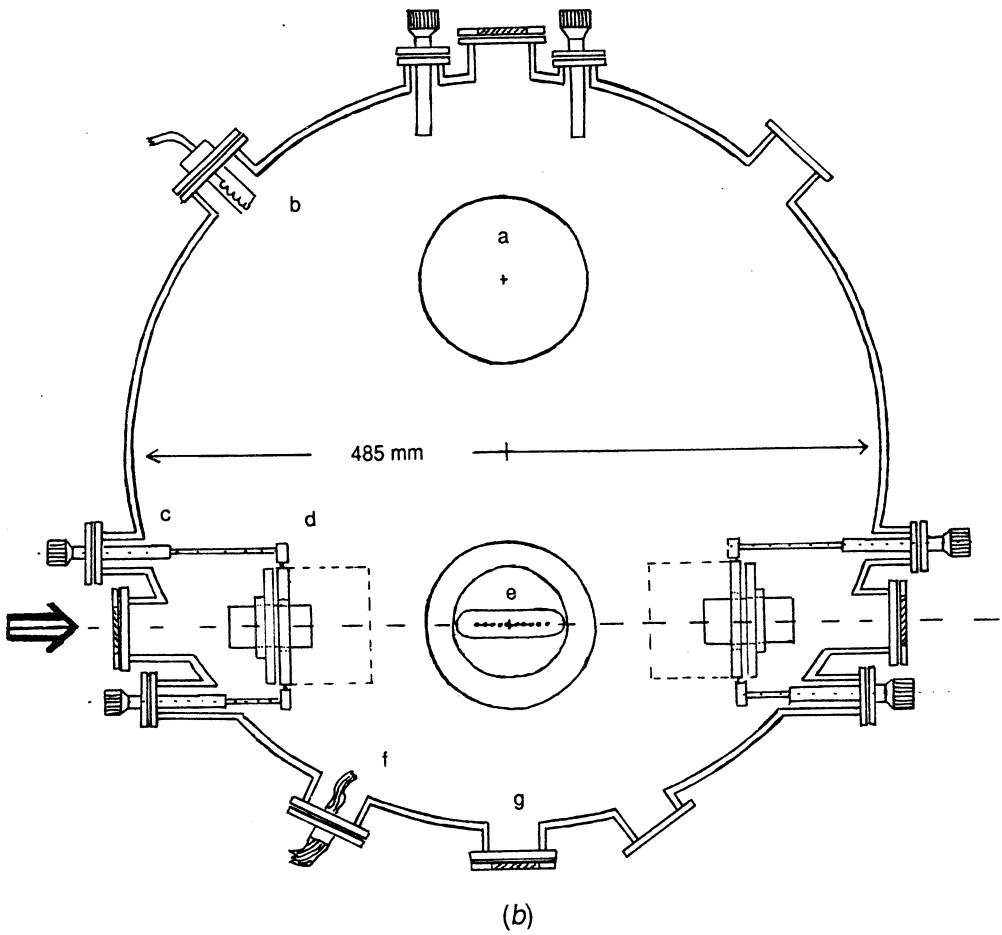

Fig. 5. (*Continued*)

the mask was made from two separate pieces of copper and 25 channels of 1 mm width were machined into the side of each piece. Hypodermic tubing was inserted into the channels and the whole assembly was silver-soldered together. Twenty-five highly parallel atomic beams were obtained. The top and bottom stages of the oven were heated separately using metal-shielded biaxial heating wire (Aerobiax Heater Cable). The temperature of various parts of the oven was monitored by copper–constantan thermocouples. The oven mounting rods were thermally insulated from the chamber base plate by machinable ceramic. The whole oven assembly, including the electrical feedthrough and all electrical connections, could be taken out from below the vacuum tank.

To test the collimation of the atomic beams, an absorption spectrum of the D_1 line was recorded in the absence of an optical cavity. The result is shown in Fig. 6. The incident laser power was approximately 14 μW in a 1 mm diameter beam in order to minimise power broadening. The resolution of

the excited level hyperfine states (frequency separation 189 MHz) suggests a residual Doppler width of approximately 200 MHz. The ground state transitions are clearly resolved. As well, the multiple atomic beam system generated sufficient atomic density at higher oven temperatures to achieve bistability.

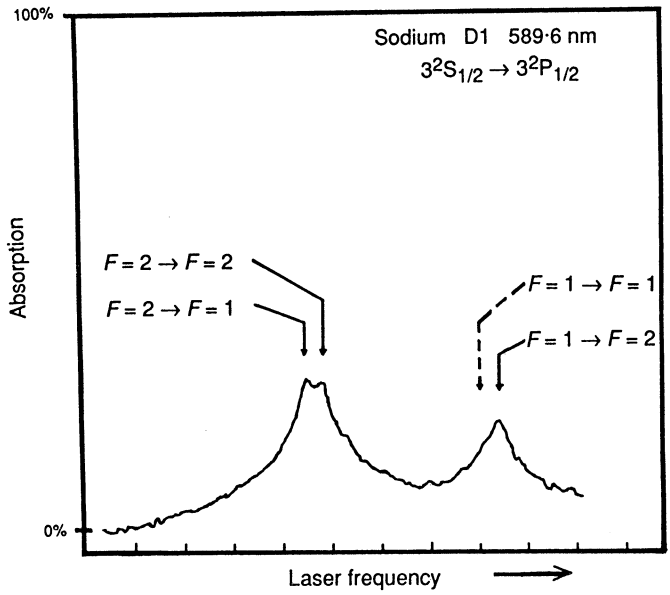

Fig. 6. Absorption spectrum of the sodium D_1 line from light transmission through the multiple atomic beams. The marker interval is 500 MHz.

Optical bistability was observed in the standard way by recording the transmitted light intensity for a complete cycle of the input intensity. For this experiment, the electro-optic switch was replaced by an Isomet 1201 E-1 40 MHz acousto-optic modulator. In the case of the Fabry–Perot etalon, an optical isolator prevented retroreflections to the modulator and the laser. The injected laser power was monitored directly in front of the entrance window to the tank by a PIN photodiode whose output was used to drive the x amplifier of the recording oscilloscope. Up to 200 mW of laser light was available at this point. By careful measurements of the system losses we estimated the intracavity light power to be twice that of the incident light. The intracavity beamwidth was typically 0·6 mm (FWHM).

Because of the frequency instability of the optical cavity, intensity sweeps were performed with a time period of about 1 ms. Most experiments were performed on the stronger D_2 line with the laser radiation typically tuned near the $3^2S_{1/2}(F'=2) \rightarrow 3^2P_{3/2}(F=3)$ hyperfine transition. Optical bistability for this laser tuning condition for various detunings of the cavity frequency of the ring cavity is shown in Fig. 7. The actual cavity detuning from the radiation frequency could not be measured. The time of the intensity cycle was approximately 200 μs.

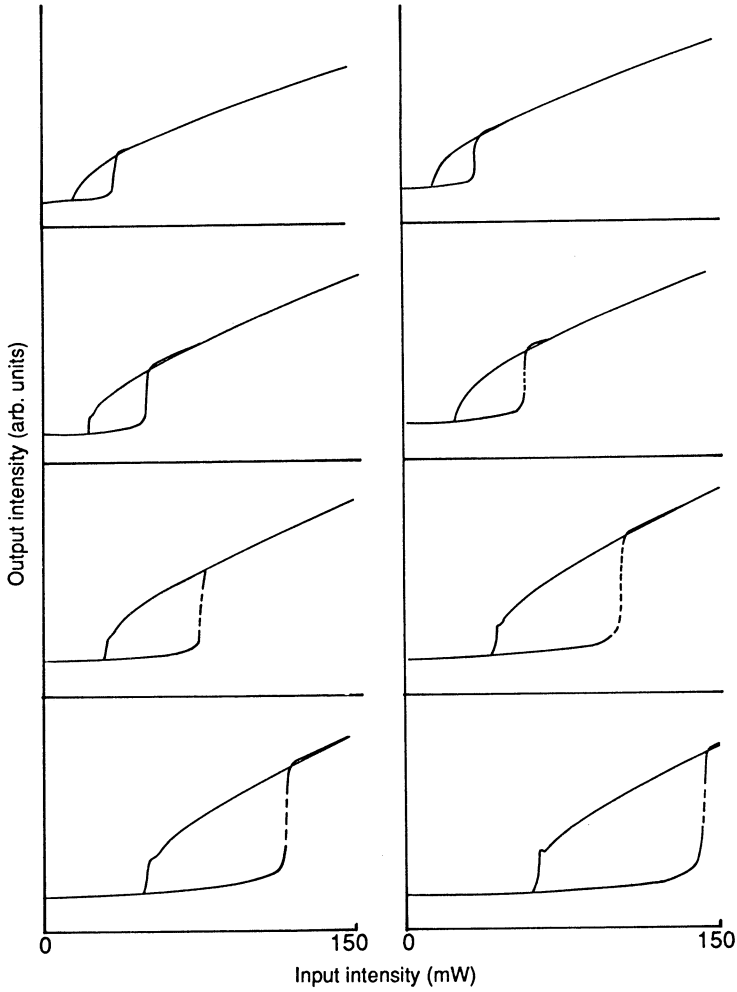

Fig. 7. Optical bistability exhibited by the ring cavity system for the laser tuned near the $3^2S_{1/2}(F'=2) \rightarrow 3^2P_{3/2}(F=3)$ hyperfine transition of the sodium D_2 line. The plots show output intensity versus input intensity as the cavity frequency was tuned through the laser frequency. The sequence starts at top left and finishes at bottom right.

So, in summary, this apparatus met the criteria of reducing the Doppler width to resolve the transitions from the hyperfine ground states while at the same time exhibiting optical bistability in a low finesse cavity.

4. Results

The responses to the light pulse of the empty cavities, the atoms alone and the complete bistable system were all investigated. Preliminary results have been published in an earlier communication (Schulz *et al.* 1984).

The response of an empty cavity to a 100 ns light pulse is shown in Fig. 8. The traces show the transmitted intensity versus time for various cavity detunings from the laser frequency. The transmissions of both types

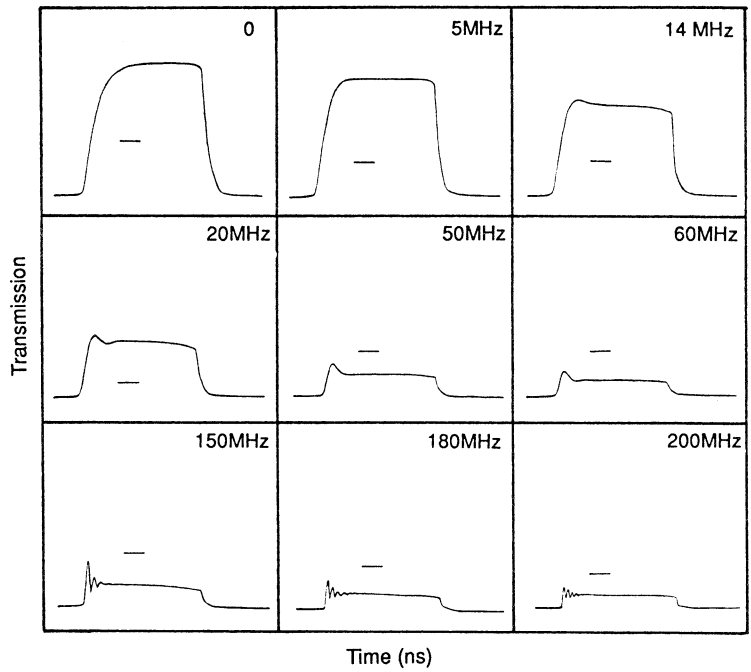

Fig. 8. Transmission of a 100 ns light pulse through an empty Fabry–Perot etalon. The y-axis scale for the bottom three traces has been expanded (×10). The length of the dash on each figure is 20 ns. A reasonable fit to the theory is obtained for $R = 0{\cdot}9$, $T = 0{\cdot}1$ and the detunings (MHz) marked in each figure.

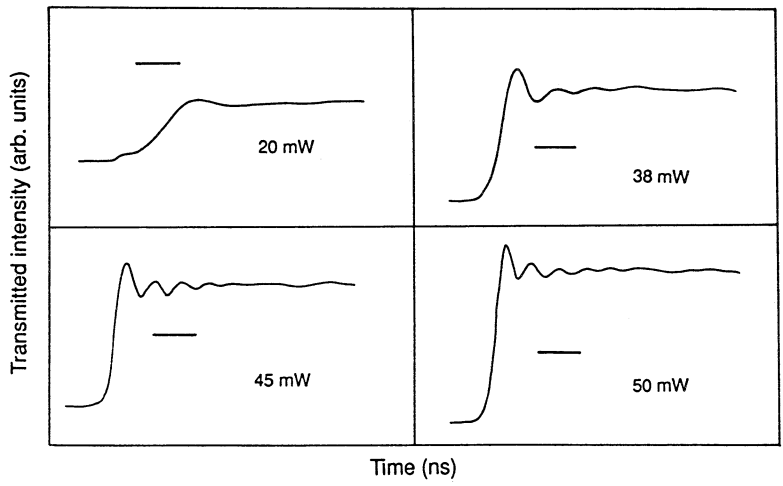

Fig. 9. Transmitted intensity response of the sodium atomic beams in the absence of a cavity to a light pulse tuned to the D_2 line $3^2S_{1/2}(F' = 2) \rightarrow 3^2P_{3/2}(F)$ transitions for various light intensities. Rabi oscillations are clearly seen. The length of the dash in each figure is 5 ns.

of cavities were obtained; the data in Fig. 8 are for the Fabry–Perot etalon. Precise measurements of the cavity detuning were not possible; however, a reasonable fit to the theory was obtained with the values listed in Fig. 8 using a reflectivity of 0·9. As in Fig. 2, an increase in the cavity detuning produced a decrease in the transmitted intensity and an increase in the frequency of the oscillations on the leading edge. From Fig. 8, it can be seen that for the on-resonance cavity, the filling time (0–90%) is approximately 20 ns which is the same order of magnitude as the atomic relaxation time of 16 ns. Thus the system is in neither the 'good' nor 'bad' cavity regime and the theory of Section 2 must be applied without further approximation.

The atomic response to the square light pulse in the absence of a cavity is illustrated in Fig. 9 where the transmitted intensity versus time is recorded for various input radiation powers. The laser light was tuned to the $3^2S_{1/2}(F'=2)\rightarrow 3^2P_{3/2}(F)$ transitions. The plots clearly show optical nutations previously observed in sodium atomic vapours (MacGillivray *et al.* 1978; Farrell *et al.* 1985). The frequency of the oscillations, the Rabi frequency, increases with the square root of the intensity (equation 3). No significant difference was found in the frequency of the oscillations when the laser was tuned to the $3^2S_{1/2}(F'=1)\rightarrow 3^2P_{3/2}(F)$ transitions. Similar results were obtained for the optical nutations associated with the transitions from the two ground states of the D_1 line. This result for each of the D lines supports the assumption in the three-level atomic model of Section 2 that the two transitions have equal dipole moments.

The decay of the oscillations in Fig. 9 is faster than that predicted by a two-level model; that is, faster than T_2 which here is 32 ns. The oscillations are also slightly non-sinusoidal indicating that the dephasing could be due to the presence of more than one discrete Rabi frequency. Different hyperfine transitions will contribute different Rabi frequencies. As well, nearly all of the transmitted beam had to be focussed onto the detector due to its low sensitivity. Thus, different parts of the beam would have contributed different Rabi frequencies according to their intensity. The residual Doppler width will also enhance the decay of the nutations.

Finally, the response of the sodium filled cavities was investigated. After first establishing that the system displayed bistability in the steady state, it was subjected to a 450 ns square light pulse. A typical set of results is shown in Fig. 10 for the Fabry–Perot etalon. The data show the transmission of the system versus time for various cavity frequency settings. The behaviour of the system was asymmetric with respect to cavity detuning indicating that the bistability was dispersive. The laser was tuned approximately to the $3^2S_{1/2}$ $(F'=2)\rightarrow 3^2P_{3/2}(F)$ transitions. All of the transmitted light was focussed on the photodiode.

The behaviour of the filled ring cavity was almost identical and transmission data for this system are displayed in Fig. 11. The system parameters for the ring cavity were approximately the same as for the Fabry–Perot etalon.

For comparison with the experimental data, transmission calculations for the ring cavity system using the model and theory of Section 2 are shown in Fig. 12. For closest agreement the injected field was modelled as being tuned 11 MHz to the high frequency side of the $|2\rangle$–$|3\rangle$ transition, that is, $\Delta'/2\pi = 11$ MHz.

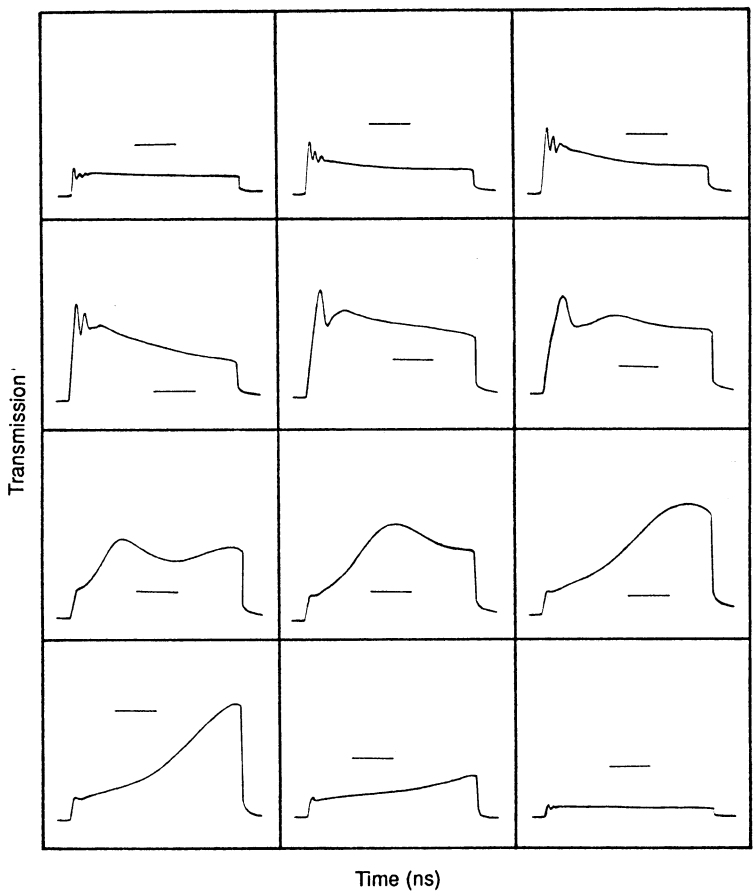

Fig. 10. Response in the transmission of the Fabry–Perot etalon system to a light pulse of approximately 450 ns duration. The laser was tuned to the $3^2S_{1/2}(F'=2) \rightarrow 3^2P_{3/2}(F)$ transitions in the sodium D_2 line. The cavity tuning was progressively changed from top left to bottom right through resonance with the laser. The length of the dash in each figure is 100 ns.

The Rabi frequency of the incident field α_i was set at $0 \cdot 1$ rad ns^{-1} and the C number was 40. The atomic relaxation times were set at $T_1 = 16$ ns, $T_2 = 32$ ns and $\tau = 1\ \mu$s. A mirror reflectivity R of $0 \cdot 8$ ($F = 14$) was used. The input pulse was modelled to have a rise time of $1 \cdot 5$ ns and to switch on at t=40 ns and off at $t = 490$ ns. With these parameter values, the agreement between the experimental and theoretical data is, qualitatively, quite good, assuming values for the cavity detuning shown in Fig. 12.

To obtain an insight into the physical processes, the simulated steady-state curves for the system parameters of Fig. 12 are given in Fig. 13. The plots show output intensity versus input intensity expressed as the square of the Rabi frequencies $|\alpha_T|$ and α_i. The value of the injected intensity used in the time-dependent simulations is marked with the dashed line. All of the plots in Fig. 13 exhibit the S-curve shape which characterises bistability. In the first plot of Fig. 13, the input intensity is well above the threshold for switch up to the high transmission branch. Even so, there is a delay of about

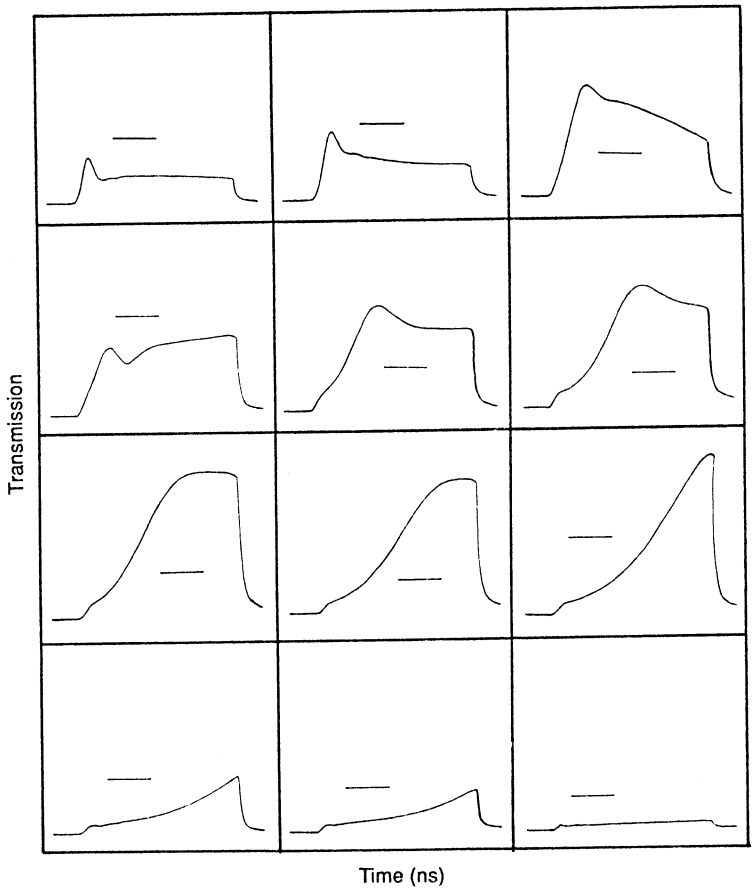

Fig. 11. Response of the ring cavity system. All details are as for Fig. 10 except that, because the free spectral range of the ring cavity is twice that of the Fabry–Perot etalon, the detuning range here is less than in Fig. 10.

100 ns in the switch up in the corresponding time response curve of Fig. 12. This delay is not as great in the relevant experimental data. Since the relative transmission of the experimental and theoretical data have been matched, the cavity detuning used in the calculations must be approximately that of the experiment and the disagreement in the switching delay may well be a product of the use of a simplified atomic level model. Note that for these relatively large values of cavity detuning the steady state in the transmission is attained quickly and in an oscillatory manner reminiscent of the detuned empty cavity.

As the cavity tuning is varied through the sequence of plots in Fig. 13, the input intensity tends towards the switch-up threshold resulting in progressively greater delay in the switch-up after the application of the light pulse until, eventually, switching does not occur even after 400 ns. This is the phenomenon of critical slowing down, previously directly observed in all-optical bistability by Grant and Kimble (1983) and Mitschke *et al.* (1983) and discussed extensively in Section 5.6 of the book by Gibbs (1985).

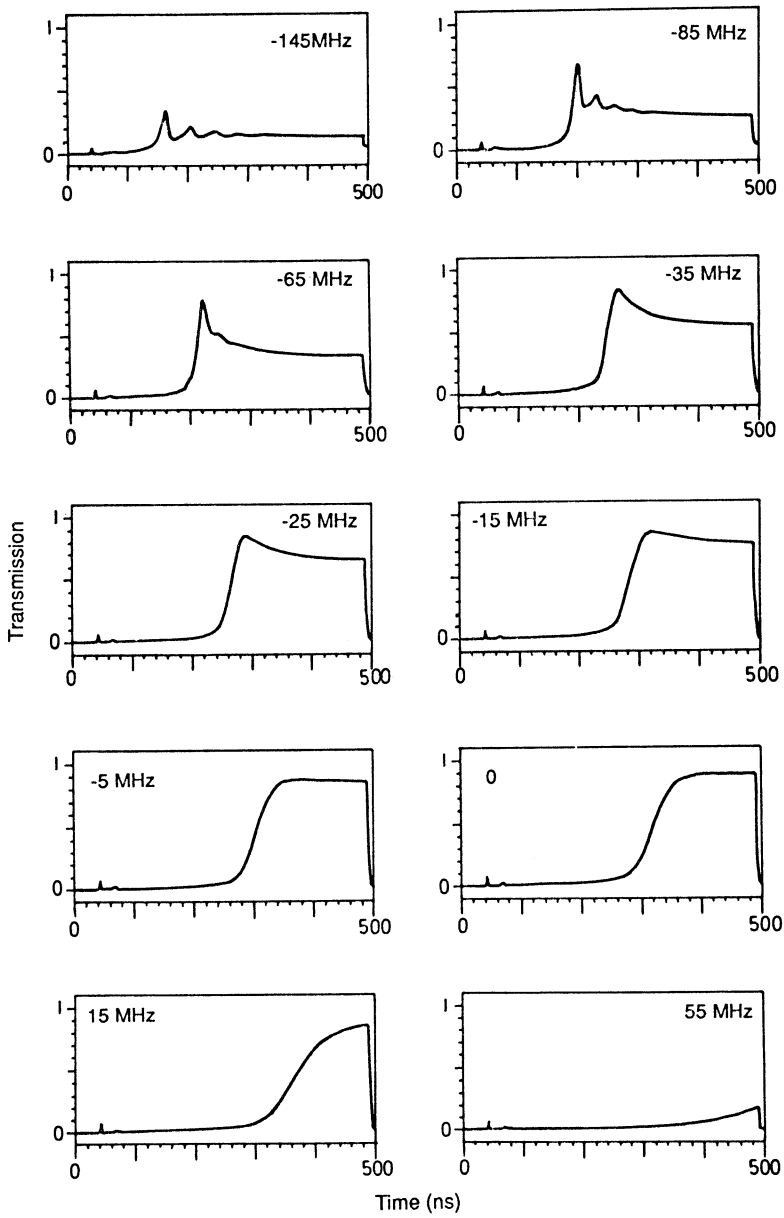

Fig. 12. Simulated ring cavity system transmission versus time for a light pulse of 1·5 ns rise time switched on at $t = 40$ ns and off at $t = 490$ ns. Here $\alpha_i = 0 \cdot 1$ rad ns^{-1}, $C = 40$, $R = 0 \cdot 8$, $T_1 = 16$ ns, $T_2 = 32$ ns and $\tau = 1$ μs. Also $\Delta'/2\pi = 11$ MHz and the cavity detunings ($\Delta_c/2\pi$) are given for each figure.

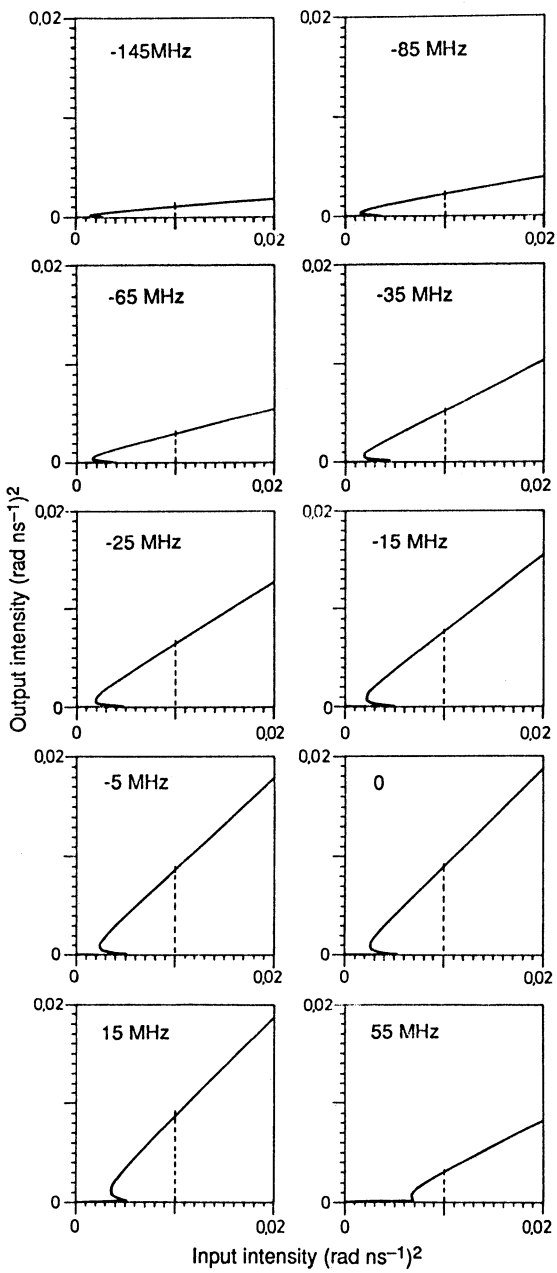

Fig. 13. Simulated output intensity versus input intensity steady-state behaviour for the parameter values of Fig. 12. The value of the injected field used in Fig. 12 is indicated by the dashed line.

5. Summary and Conclusions

We have described in some detail an apparatus that exhibits the property of optical bistability in which the lifetimes of the cavity field and medium are approximately equal. The response of this system to a square light pulse has been recorded experimentally and compared with computer simulations of a theory in which the atomic medium is modelled as having a three-level lambda-type energy configuration. Since neither the field nor atomic lifetimes can be adiabatically eliminated, the coupled differential equations describing the time evolution of each had to be solved simultaneously subject to the cavity boundary conditions. Comparison of the observed and simulated transmissions displayed good qualitative agreement. In particular, critical slowing down in the switching of the system to the high transmission branch has been clearly demonstrated.

The apparatus could be improved in two principal areas. Firstly, a more sensitive detector is needed. A fast photomultiplier tube should replace the PIN photodiode so that light from only the uniformly intense central portion of the transmitted beam is collected. This would reduce the range of effective Rabi frequency components detected. Secondly, the optical cavity should be stabilised so that the accurate measurements of cavity detuning may be made. This exercise is currently being undertaken. It would be interesting to extend this study to a bistable system in the 'bad cavity' limit. This would allow the atomic behaviour to dominate that of the cavity. However, to reach this regime would require a considerable reduction in cavity finesse. To maintain bistability, the atomic number density would have to be correspondingly increased. This may lead to technical difficulties. Alternatively, another atomic transition with a longer lifetime may be employed. However, the lower Rabi frequency may remove the system from the bistable regime, again making an increase in the atomic number density a necessity.

Acknowledgments

One of us (W.E.S.) was the holder of a Griffith University Postgraduate Research Award. We acknowledge the financial assistance of the Australian Research Grants Scheme.

References

Abate, J. A. (1974). *Opt. Commun.* **10**, 269.
Abraham, E., and Smith, S. D. (1982). *Rep. Prog. Phys.* **45**, 815.
Allen, L., and Eberly, J. H. (1975). 'Optical Resonance and Two-level Atoms' (Wiley: New York).
Alzetta, G., Moi, L., and Orriols, G. (1979). *Nuovo Cimento* B **52**, 209.
Arecchi, F. T., Giusfredi, G., Petriella, E., and Salieri, P. (1982). *Appl. Phys.* B **29**, 79.
Ballagh, R. J., Cooper, J., and Sandle, W. J. (1981). *J. Phys.* B **14**, 3881.
Bonifacio, R., and Lugiato, L. A. (1976). *Opt. Commun.* **19**, 172.
Bonifacio, R., and Meystre, P. (1978). *Opt. Commun.* **27**, 147.
Farrell, P. M., MacGillivray, W. R., and Standage, M. C. (1985). *Phys. Lett.* A **107**, 263.
Gawlik, W., and Zachorowski, J. (1987). *J. Phys.* B **20**, 5939.
Gibbs, H. M. (1985). 'Optical Bistability: Controlling Light with Light' (Academic: Orlando).
Gibbs, H. M., McCall, S. L., and Venkatesan, T. N. C. (1976). *Phys. Rev. Lett.* **36**, 1135.
Grant, D. E., and Kimble, H. J. (1982). *Opt. Lett.* **7**, 353.
Grant, D. E., and Kimble, H. J. (1983). *Opt. Commun.* **44**, 415.

Kimble, H. J., Grant, D. E., Rosenberger, A. T., and Drummond, P. D. (1983). *In* 'Laser Physics' (Eds J. D. Harvey and D. F. Walls), Lecture Notes in Physics Vol. 182, p. 40 (Springer: Berlin).
Lugiato, L. A. (1983). *Contemp. Phys.* **24**, 333.
MacGillivray, W. R., Pegg, D. T., and Standage, M. C. (1978). *Opt. Commun.* **25**, 355.
McCall, S. L. (1974). *Phys. Rev.* A **9**, 1515.
Mitschke, F., Deserno, R., Mlynek, J., and Lange, W. (1983). *Opt. Commun.* **46**, 135.
Mlynek, J., Mitschke, F., Deserno, R., and Lange, W. (1984). *Phys. Rev.* A **29**, 1297.
Orozco, L. A., Kimble, H. J., and Rosenberger, A. T. (1987*b*). *Opt. Commun.* **62**, 54.
Orozco, L. A., Raizen, M. G., Xiao, M., Brecha, R. J., and Kimble, H. J. (1987*c*). *J. Opt. Soc. Am.* B **4**, 1490.
Orozco, L. A., Rosenberger, A. T., and Kimble, H. J. (1984). *Phys. Rev. Lett.* **53**, 2547.
Orozco, L. A., Rosenberger, A. T., and Kimble, H. J. (1987*a*). *Phys. Rev.* A **36**, 3248.
Orriols, G. (1979). *Nuovo Cimento* B **53**, 1.
Pegg, D. T., and Schulz, W. E. (1985). *Opt. Commun.* **53**, 274.
Raizen, M. G., Orozco, L. A., Xiao, M., Boyd, T. L., and Kimble, H. J. (1987). *Phys. Rev. Lett.* **59**, 198.
Rosenberger, A. T., Orozco, L. A., and Kimble, H. J. (1983). *Phys. Rev.* A **28**, 2569.
Rosenberger, A. T., Orozco, L. A., and Kimble, H. J. (1984). *In* 'Fluctuations and Sensitivity in Nonequilibrium Systems' (Eds W. Horsthemke and D. K. Kondepudi), p. 62 (Springer: Berlin).
Sandle, W. J., and Gallagher, A. (1981). *Phys. Rev.* A **24**, 2017.
Schulz, W. E., MacGillivray, W. R., and Standage, M. C. (1983). *Opt. Commun.* **45**, 67.
Schulz, W. E., MacGillivray, W. R., and Standage, M. C. (1984). *Phil. Trans. R. Soc. Lond.* A **313**, 227.
Schulz, W. E., MacGillivray, W. R., and Standage, M. C. (1987). *Phys. Rev.* A **36**, 1316.
Smith, S. D., Walker, A. C., Tooley, F. A. P., and Wherett, B. S. (1987). *Nature* **325**, 27.
Szöke, A., Daneu, Y., Goldhar, J., and Kurnit, N. A. (1969). *Appl. Phys. Lett.* **15**, 376.
Weyer, K. G., Wiedenmann, H., Rateike, M., MacGillivray, W. R., Meystre, P., and Walther, H. (1981). *Opt. Commun.* **37**, 426.

Manuscript received 5 September 1988, accepted 13 January 1989